Ultra-Wideband Multicarrier Communication Receiver Based on Analog to Digital Conversion in the Frequency Domain

Sebastian Hoyos†, Brian M. Sadler‡, Gonzalo R. Arce♮

†University of California, Berkeley
Department of EECS
Berkeley, CA
hoyos@eecs.berkeley.edu

‡Army Research Laboratory
AMSRD-ARL-CI-CN
Adelphi, MD
bsadler@arl.army.mil

♮University of Delaware
Department of ECE
Newark, DE
arce@ee.udel.edu

***Abstract*— This paper introduces an ultra-wideband multicarrier communication receiver based on analog to digital conversion (ADC) in the frequency domain. The samples of the spectrum of the received signal are used in the digital receiver to estimate the transmitted symbols through a matched filter operation in the discrete frequency domain. The proposed receiver is aimed at the reception of high information rates in a multicarrier signal with very large bandwidth. Thus, the receiver architecture provides a solution to some of the challenging problems found in the implementation of conventional wideband multicarrier receivers based on time-domain ADC, since it parallelizes the A/D conversion reducing the sampling rate. The receiver is also directly applicable to multicarrier ultra-wideband communication receivers. Additional advantages of the proposed receiver include the possibility of optimally allocating the available number of bits for the A/D conversion across the frequency domain samples, narrowband interference suppression that can be directly carried out in the frequency domain, and inherent robustness to frequency offset which makes it an attractive solution when compared with traditional multicarrier receivers.**

I. Introduction

In multicarrier communications systems, the available channel bandwidth is efficiently used by subdividing it into a number of subchannels with sufficiently small bandwidth such that each subchannel frequency response is non-frequency selective [1–3]. Therefore, the extent of inter-symbol interference (ISI) is greatly reduced and the available transmit power can be optimally allocated across the subchannels in order to optimize throughput [4]. Such systems have been successfully implemented, with orthogonal frequency division multiplexing (OFDM) the most well-known approach [5–7]. The OFDM receiver architecture is essentially based on conventional time-domain analog to digital conversion followed by a discrete Fourier transform (DFT) that provides the estimates of the transmitted symbols. However, if the bandwidth of the multicarrier signal is increased in order to achieve higher data rates and accommodate larger numbers of users, the implementation of the front-end conventional time-domain ADC operating at Nyquist rate presents a significant challenge. This technological limitation has constrained the instantaneous transmission bandwidth employed for the multicarrier signal, which in turn limits the data transmission rates even if higher bandwidths are available. An example of this limitation is the implementation of ultra-wideband communication systems based on multicarrier technology, where even though a bandwidth of 9.5 GHz is available for the transmission of information, proposed systems use the minimum instantaneous bandwidth of 500 MHz allowed by the FCC [8, 9].

The multicarrier receiver presented in this paper provides a solution that parallelizes the analog to digital conversion, efficiently reducing the operational speed of the ADC even if signals with very large bandwidths are used for the transmission of high data rates. The new receiver architecture is based on an analog to digital converter in the frequency domain [10–12] that takes N samples of the spectrum of the received signal every T_c seconds. The samples of the signal spectrum are used in a digital receiver based on a bank of discrete-frequency matched filters that calculate the estimates of the transmitted symbols. The proposed receiver possesses additional advantages such as the possibility of optimally allocating the available number of bits used in the quantization of the frequency samples, an inherent robustness to frequency offset, and the direct application of narrow band interference suppression methods in the frequency domain.

II. Analog to Digital Conversion in the Frequency Domain

Figure 1(a) shows the block diagram of the ADC in the frequency domain [10] in which signal projection over the complex exponential functions allows sampling of the continuous-time signal spectrum at the frequencies $F_n \mid_{n=0}^{N-1}$, leading to the set of frequency coefficients

$$c_n = \int_0^{T_c} s(t) e^{-j2\pi F_n t}\, \mathrm{d}t, \qquad n = 0, \cdots, N-1. \quad (1)$$

The coefficients $c_n \mid_{n=0}^{N-1}$ are then quantized by a set of quantizers $Q_n \mid_{n=0}^{N-1}$, which in turn produce the ADC output digital coefficients $\hat{c}_n = Q_n(c_n) \mid_{n=0}^{N-1}$. The conversion frequency sample spacing $\Delta F_c = F_n - F_{n-1}$ complies with $\Delta F_c \leq \frac{1}{T_c}$

Prepared through collaborative participation in the Communications and Networks Consortium sponsored by the U. S. Army Research Laboratory under the Collaborative Technology Alliance Program, Cooperative Agreement DAAD19-01-2-0011.

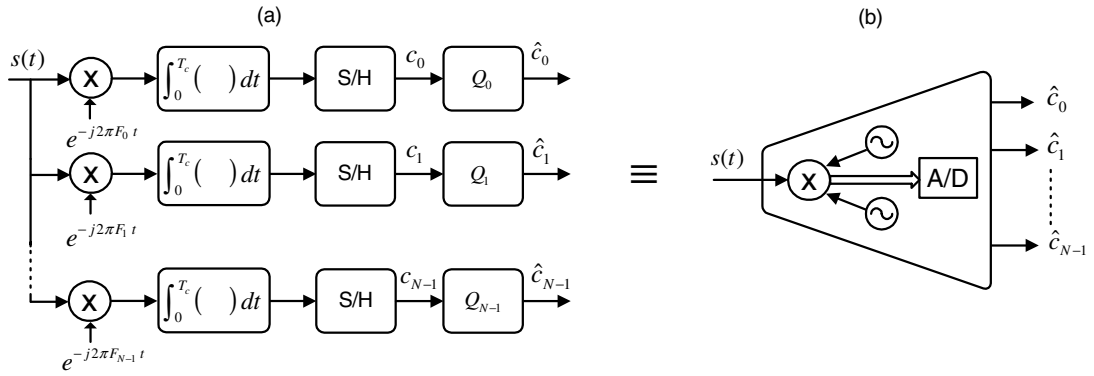

Fig. 1. (a) Block diagram of the analog to digital converter in the frequency domain. (b) Block representation of the ADC in the frequency domain.

in order to avoid aliasing in the discrete-time domain. Thus, the optimal number of coefficients N necessary to fully sample the signal spectrum with bandwidth W is given by

$$N = \left\lceil \frac{W}{\Delta F_c} \right\rceil \geq \lceil W T_c \rceil, \tag{2}$$

where the operator $\lceil\ \rceil$ is used to ensure that N is the closest upper integer that avoids discrete-time aliasing.

A. A/D Conversion of Multicarrier Signals in the Frequency Domain

Let us consider the complex envelope of a multicarrier signal $x(t)$ composed of the sum of S complex exponentials with associated complex amplitude $a_s\ |_{s=0}^{S-1}$

$$x(t) = \sum_{s=0}^{S-1} a_s e^{j2\pi f_s t}, \qquad 0 \leq t \leq T, \tag{3}$$

where the intercarrier frequency spacing is given by $\Delta F = f_s - f_{s-1} = \frac{1}{T}\ \forall s$. We first notice that by making $T_c = T$, a total of $N = S$ frequency samples of $x(t)$ are needed to recover the coefficients $a_s\ |_{s=0}^{S-1}$. In such a case, the frequency domain ADC is just a simple correlator bank. The problem with choosing $T_c = T$ is that when a large number of carriers are used, twice this number of multiply and integrate devices are needed in the implementation of the correlator bank, which could make the system impractical. Therefore, it is of great interest to investigate cases in which the conversion-time satisfies $T_c < T$. In particular, we chose $T_c = T/M$, with M an integer. We define the signal $x_m(t) = x(t)w_m(t)$,

$$w_m(t) = \begin{cases} 1 & mT_c \leq t \leq (m+1)T_c \\ 0 & \text{elsewhere} \end{cases} \tag{4}$$

where $m = 0, \cdots, M-1$, and the window $w_m(t)$ has been selected as rectangular for simplicity of the analysis. It is easy to verify that the Fourier transform ($\mathcal{F}$) of $w_m(t)$ is given by $\mathcal{F}\{w_m(t)\} = W_m(F) = \frac{\sin(\pi F T_c)}{\pi F} e^{-j\pi(2m+1)T_c F}$. The Fourier transform of $x_m(t)$, denoted as $X_m(F)$, can be expressed as

$$\begin{aligned} X_m(F) &= \mathcal{F}\{x(t)\} * \mathcal{F}\{w_m(t)\} = \mathcal{F}\left\{\sum_{s=0}^{S-1} a_s e^{j2\pi f_s t}\right\} * W_m(F) \\ &= \left(\sum_{s=0}^{S-1} a_s \delta(F - f_s)\right) * \left(\frac{\sin(\pi F T_c)}{\pi F} e^{-j\pi(2m+1)T_c F}\right) \\ &= \sum_{s=0}^{S-1} a_s \frac{\sin(\pi T_c (F - f_s))}{\pi (F - f_s)} e^{-j\pi T_c (2m+1)(F - f_s)}, \end{aligned} \tag{5}$$

The spectrum in (5) is sampled every $\Delta F_c = \frac{1}{T_c}$ Hz. A total of N samples are taken based on Eqn. (2). The bandwidth W changes depending on the segmentation ratio $M = T/T_c$. Figure 2 (a) illustrates the bandwidth expansion that $X_m(F)$ experiences due to time windowing. The figure shows that with no windowing, the multicarrier signal occupies a bandwidth equal to $S\Delta F$[1], while windowing introduces a bandwidth expansion equal to $\frac{T - T_c}{T_c}\Delta F$. Thus, the bandwidth W is given by

$$\begin{aligned} W &= S\Delta F + \frac{T - T_c}{T_c}\Delta F \\ &= S\Delta F + \left(\frac{\Delta F_c}{\Delta F} - 1\right)\Delta F \\ &= (S + M - 1)\,\Delta F \end{aligned} \tag{6}$$

Additionally, based on Eqn. (2), the number of frequency samples N is given by

$$\begin{aligned} N &= \left\lceil (S + M - 1)\,\frac{\Delta F}{\Delta F_c} \right\rceil \\ &= \left\lceil \frac{S}{M} + \frac{M - 1}{M} \right\rceil \end{aligned} \tag{7}$$

Note also that if no bandwidth expansion is taken into account, Eqn. (7) reduces to $N = S/M$. These equations show that

[1]This bandwidth accounts only for the range of frequencies occupied by the main lobe of the carriers.

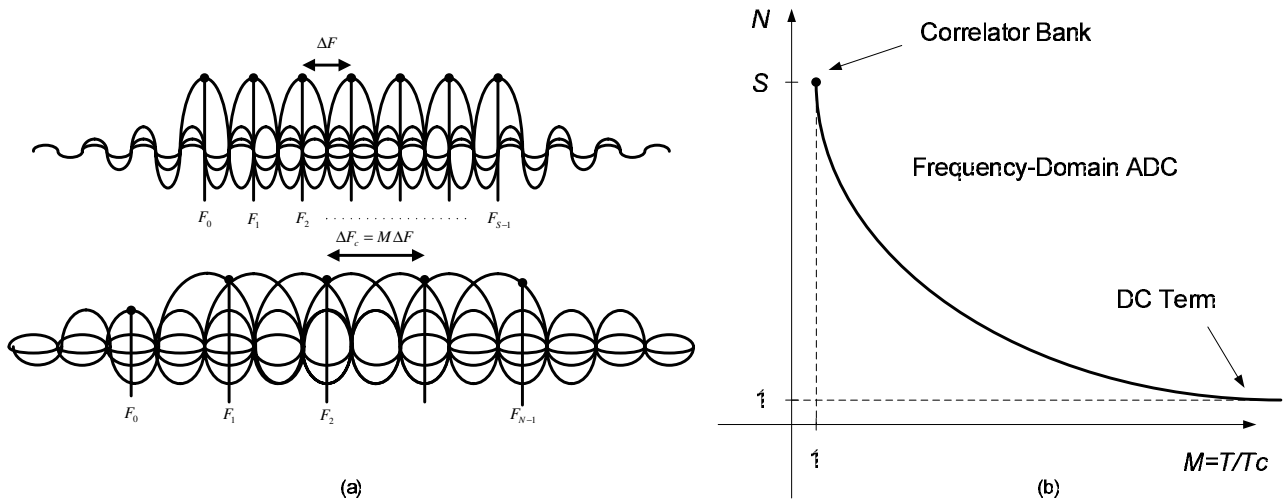

Fig. 2. Characteristics of A/D conversion of multicarrier signals in the frequency domain. (a) Effect of time segmentation in the bandwidth of the multicarrier signal and in the samples frequency spacing ΔF_c. (b) Number of coefficients N versus the symbol-period to segmentation-time ratio ($M = T/T_c$).

although the bandwidth of all the individual carriers that compose $x(t)$ is inversely proportional to T_c, only the changes in the bandwidth of the carriers that lie at the edges of the spectrum of the multicarrier signal will affect the overall bandwidth. Although some truncation error will occur here, N and M can be adequately chosen to achieve some desired performance. The inner carriers' spectrum will also spread out, overlapping the neighbor carriers, but will not increase the bandwidth of $x(t)$. Although the carriers are no longer orthogonal within each segment for a conversion-time $T_c < T$, we show in section III-A that no intercarrier interference (ICI) is introduced when the receiver processes all the segments to calculate the symbols estimates.

This simple result represents a fundamental concept in the development of the ideas presented in this paper. The result shows us that even though further segmentation of the multicarrier signal increases the bandwidth of the signal to be A/D converted, an even larger reductions in the number of coefficients N is obtained. The favorable trade-off between N and T_c is very important in the implementation of the ADC in the frequency domain for multicarrier signals, since it indicates that a practical number of frequency samples N can be obtained by adequately selecting a symbol-period to conversion-time ratio $M = T/T_c$.

Additionally, it is interesting to notice that as $M = T/T_c$ is increased, the number of frequency samples N will eventually reach the value 1, which is just the point where the ADC in the frequency domain turns into a zero-frequency term of the transform. At this point of operation, the ADC samples the DC frequency, which is just the average of the signal over the integration time T_c. Furthermore, if T_c is decreased further, the signal in the interval T_c approaches a flat level, which turns the ADC into a conventional time-domain ADC with some degree of oversampling. So, Fig. 2(b) illustrates the three regions of operation of the ADC of Fig. 1, which are (1) $T_c = T$ which leads to $N = S$, a straightforward correlator bank, which not suffers from truncation error (2) $T_c < T$ such that $N < S$, which is the proposed ADC in the frequency domain and (3) $T_c << T$ such that $N = 1$, the DC term in the Fourier transform which can turn into a conventional time-domain ADC if a sufficient oversampling rate is allowed, i.e. T_c smaller than the Nyquist sampling period.

III. Multicarrier Communication System Based on Frequency Domain A/D Conversion

Assume that the available channel bandwidth BW is divided into S subchannels of bandwidth BW/S with center frequencies $f_s\ |_{s=0}^{S-1}$. Thus, a block of S symbols $a_s\ |_{s=0}^{S-1}$ is simultaneously transmitted through the channel over a signal block time T. The transmitted signal for a block of symbols can be expressed as in Eqn. (3). In OFDM systems, the generation of the transmit signal $x(t)$ is achieved by performing an inverse DFT operation over the block of symbols $a_s\ |_{s=0}^{S-1}$, which are then passed through a D/A converter to generate a continuous-time signal that is then frequency shifted to some desired frequency band.

The signal $x(t)$ is transmitted over a linear communication channel with impulse response $h(t)$ and frequency response $H(f)$. Assuming that the channel is flat in each of the transmission subbands, the received signal can be expressed as follows

$$r(t) = x(t) * h(t) + z(t) \approx \sum_{s=0}^{S-1} a_s e^{j2\pi f_s t} H(f_s) + z(t),\ 0 \le t \le T. \tag{8}$$

where "$*$" indicates continuous-time convolution and $z(t)$ is additive white Gaussian noise (AWGN). In conventional OFDM systems, the received continuous-time signal is first passed through a time-domain A/D converter running at

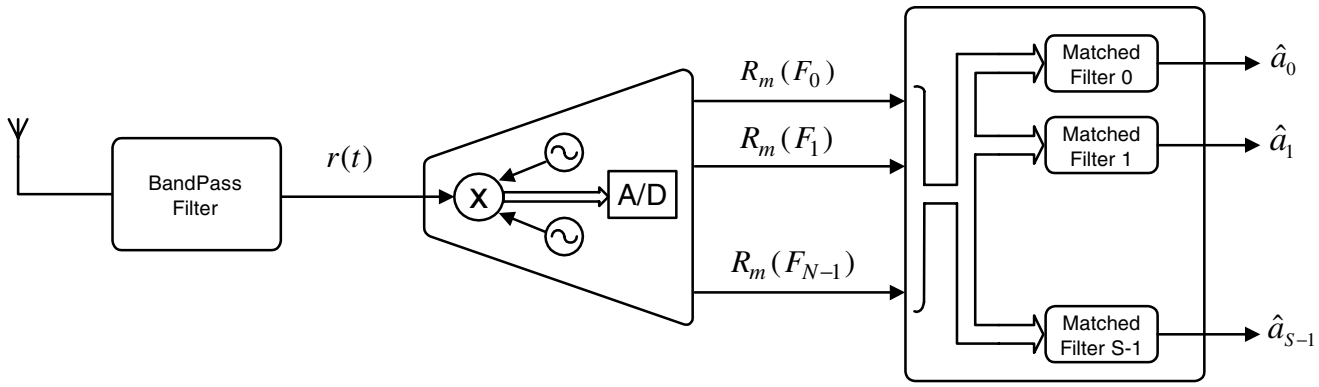

Fig. 3. Block diagram of multicarrier receiver based on ADC in the frequency domain.

Nyquist rate, and the discrete-time samples are then demodulated by performing a DFT operation. The following subsection presents a fundamentally different approach for the implementation of the multicarrier receiver, based on A/D conversion in the frequency domain.

A. Multicarrier Receiver Based on Analog to Digital Conversion in the Frequency Domain

Figure 3 illustrates the proposed receiver architecture. The ADC in the frequency domain provides the set of samples $R_m(F_n)\ |_{n=0}^{N-1}$ every T_c seconds, where $m = 0, \cdots, M-1$ and the information symbol block period T is related with the A/D conversion-time T_c as $T = MT_c$. We begin by expressing the calculation as a matched filter problem in time domain $\bar{a}_s = \int_0^T r(\tau) g_s^*(\tau)\ \mathrm{d}\tau$, where $\bar{a}_s$ is the estimated symbol associated to the carrier at frequency f_s, $g(t)$ is the impulse response of the matched filter and the output of this filter is sampled at $t = T$. Ideally, the matched filter impulse response is given by

$$g_s^*(t) = e^{-j2\pi f_s t} * h^*(t) \approx e^{-j2\pi f_s t} H^*(f_s),\ 0 \le t \le T \qquad (9)$$

where $(\cdot)^*$ indicates complex conjugate, and once again the approximation follows from assuming that the channel frequency response is flat across the subchannels. In order to reflect the effect of segmenting the signal duration time T into M timeslots of duration T_c, we define the following signals

$$r_m(t) = r(t) w_m(t), \quad g_{s,m}(t) = g_s(t) w_m(t), \qquad (10)$$

where $m = 0, \cdots, M-1$, and the window $w_m(t)$ is introduced in (4). Using these definitions, the matched filter output can be expressed as

$$\bar{a}_s = \sum_{m=0}^{M-1} \int_{mT_c}^{(m+1)T_c} r(\tau) g_s^*(\tau)\ \mathrm{d}\tau \qquad (11)$$
$$= \sum_{m=0}^{M-1} \int_{mT_c}^{(m+1)T_c} r_m(\tau) g_{s,m}^*(\tau)\ \mathrm{d}\tau = \sum_{m=0}^{M-1} \int_{-\infty}^{\infty} r_m(\tau) g_{s,m}^*(\tau)\ \mathrm{d}\tau,$$

In order to express the matched filter operations in the frequency-domain, the Parseval's theorem is used in (11), leading to

$$\bar{a}_s = \sum_{m=0}^{M-1} \int_{-\infty}^{\infty} r_m(\tau) g_{s,m}^*(\tau)\ \mathrm{d}\tau$$
$$= \sum_{m=0}^{M-1} \int_{-\infty}^{\infty} R_m(F) G_{s,m}^*(F)\ \mathrm{d}F, \qquad (12)$$

where $R_m(F) = \mathcal{F}\{r_m(t)\}$ and $G_{s,m}(F) = \mathcal{F}\{g_{s,m}(t)\}$. Since only N samples of the received signal spectrum are provided by the ADC in the frequency domain, (12) is approximated as

$$\bar{a}_s = \sum_{m=0}^{M-1} \int_{-\infty}^{\infty} R_m(F) G_{s,m}^*(F)\ \mathrm{d}F \qquad (13)$$
$$\approx \sum_{m=0}^{M-1} \Delta F_c \sum_{n=0}^{N-1} \left(R_m(F_n) G_{s,m}^*(F_n) + R_m(-F_n) G_{s,m}^*(-F_n) \right),$$

where $R_m(\pm F_n)\ |_{n=0}^{N-1}$ and $G_{s,m}(\pm F_n)\ |_{n=0}^{N-1}$ are the samples from the spectrum of $r_m(t)$ and $g_{s,m}(t)$, respectively. Since the received signal is real-valued, we have that $R_m(F_n) = R_m^*(-F_n)$. If the number of frequency samples K, where $K = 2(N-1)$, comply with both no discrete-time aliasing and Nyquist rate, the error introduced in (13) is negligible.

The samples of the spectrum of the segmented matched filter, $G_{s,m}^*(F_n)\ |_{n=0}^{N-1}$, need to be estimated in order to calculate the information symbol estimates in (13). The accuracy of the estimates $\hat{a}_s$ will depend on how close the channel estimates $\hat{G}_{s,m}(F_n)\ |_{n=0}^{N-1}$ are to their true values $G_{s,m}(F_n)\ |_{n=0}^{N-1}$. When the channel estimates are perfect, the signal is free of intercarrier or intersymbol interference, and the number of spectrum samples N satisfies Eqn. (2) which avoids discrete-time aliasing and makes the error in (12) negligible, then the probability of error associated with this receiver will be the same probability of error of a conventionally implemented multicarrier or multichannel communication system.

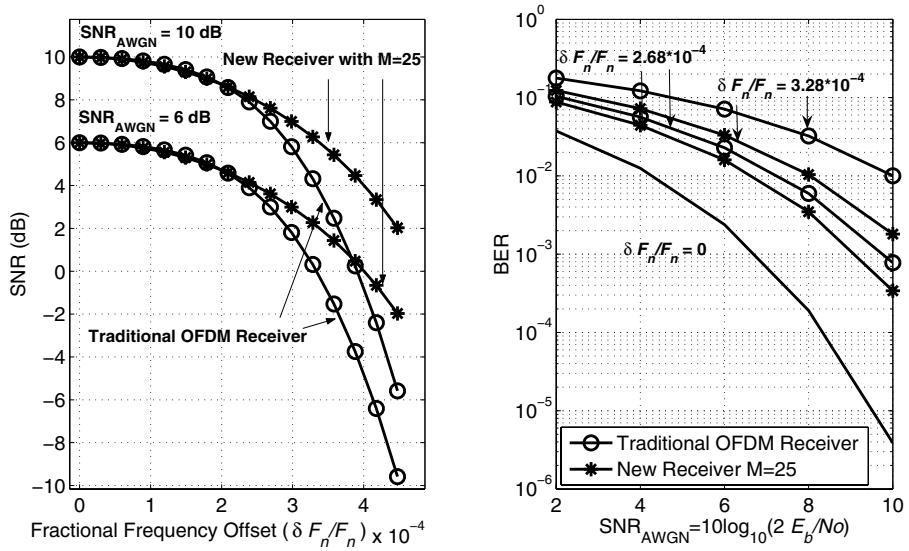

Fig. 4. Impact of frequency offset on the performance of multicarrier receiver. (a) SNR vs. fractional frequency offset ($\delta F_n/F_n$) for $M = 1$ and $M = 25$. (b) BER vs. $\mathrm{SNR}_{\mathrm{AWGN}} = 10\log_{10}(E_s/N_o)$ for fractional frequency offsets $\delta F_n/F_n = 0$, $\delta F_n/F_n = 2.68 * 10^{-4}$, $\delta F_n/F_n = 3.28 * 10^{-4}$.

IV. System Advantages and System and Channel Impairments

A. Channel Estimation

The estimation of the information symbols in (13) requires the calculation of the matched-filter coefficient estimates $\hat{G}_{s,m}(F_n)$. In order to obtain these estimates, we begin by explicitly expressing the Fourier transform of time-segmented matched filters

$$\begin{aligned}\mathcal{F}\{g_{s,m}(t)\} &= G_{s,m}(F) = \mathcal{F}\{g_s(t)w_m(t)\} \\ &= G_s(F) * W_m(F) = [H(f_s)\delta(F-f_s)] * W_m(F) \\ &= H(f_s)W_m(F-f_s) \\ &= H(f_s)\frac{\sin(\pi T_c(F-f_s))}{\pi(F-f_s)}e^{-j\pi T_c(2m+1)(F-f_s)}. \quad (14)\end{aligned}$$

The only unknown variable in (14) is the channel coefficient $H(f_s)$, which can be estimated by using training. A maximum likelihood (ML) estimate of $H(f_s)$ can be obtained by sending a known set of symbols $a_{s,i}\,|_{i=0}^{I-1}$, through the transmission of I independent blocks. At the receiver, the frequency samples $R_{m,i}(F_n)\,|_{n=0}^{N-1}\,|_{i=0}^{I-1}\,|_{m=0}^{M-1}$ are given by

$$\begin{aligned}R_{m,i}(F_n) = &\sum_{s=0}^{S-1} a_{s,i}H(f_s)\frac{\sin(\pi T_c(F_n-f_s))}{\pi(F_n-f_s)}e^{-j\pi T_c(2m+1)(F_n-f_s)} \\ &+ Z_{m,i}(F_n), \quad (15)\end{aligned}$$

where $Z_{m,i}(F_n) = \int_{-\infty}^{\infty} z_i(t)w_m(t)e^{j2\pi F_n t}\,\mathrm{d}t$ are just the noise frequency samples, with $z_i(t)$ the AWGN realization associated with the ith block of symbols.

The received signal frequency samples are correlated as indicated in (13) against the marginal matched filter samples $\tilde{G}_{m,s,}(F_n) = W_m(F_n - f_s)\,|_{n=0}^{N-1}\,|_{m=0}^{M-1}$, which are just the optimal matched filter samples from (14) with $H(f_s) = 1$, leading to the following estimates

$$\begin{aligned}\tilde{a}_{s,i} = &\sum_{m=0}^{M-1}\Delta F_c\sum_{n=0}^{N-1}\left(R_{m_i}(F_n)\tilde{G}^*_{s,m}(F_n) + R^*_{m_i}(F_n)\tilde{G}^*_{s,m}(-F_n)\right) \\ &\approx a_{s,i}H(f_s) + Z_i, \qquad i = 0,\cdots,I-1. \quad (16)\end{aligned}$$

where Z_i is the noise component at the output of the matched filter which can be modelled as AWGN. It is assumed in (16) that the channel remains constant during the I blocks used in the estimate, and any remaining inter-block interference in the received signal has been taken care of by either introducing a time-gap, or cyclic prefix or suffix between adjacent blocks of symbols. The ML estimate of the channel coefficient can be readily obtained from (16) although it is omitted here; blind estimation methods are also possible.

B. Frequency Offset

In this section we study the impact on the receiver performance of frequency offset introduced by some channel and system perturbations. This corruptive phenomena can be quantified by expressing the received signal $r(t)$ and local oscillators $O_n(t)\,|_{n=0}^{N-1}$ as follows

$$r(t) = \left(\sum_{s=0}^{S-1} a_s H(f_s)e^{j2\pi f_s t}\right)e^{j\theta(t)} + z(t), \quad (17)$$

$$O_n(t) = e^{-j2\pi F_n t}e^{j\phi_n(t)}, \quad (18)$$

where $\theta(t)$ and $\phi_n(t)$ are deterministic and given by $\theta(t) = 2\pi\delta\bar{f}t + \Theta$ and $\phi_n(t) = 2\pi\delta f_n + \Phi_n$, where $\delta\bar{f}$ and δf_n are the frequency offsets. We express the frequency samples $R_m(F_n)\,|_{n=0}^{N-1}$ as follows

$$\begin{aligned}R_m(F_n) &= \int_{-\infty}^{\infty} r_m(t)O_n(t)\,\mathrm{d}t \\ &= \int_{-\infty}^{\infty}\left[\left(\sum_{s=0}^{S-1}H(f_s)a_s e^{j2\pi f_s t}e^{j\theta(t)} + z(t)\right)w_m(t)\right]e^{-j2\pi F_n t}e^{j\phi_n(t)}\,\mathrm{d}t \\ &= \sum_{s=0}^{S-1}H(f_s)a_s\int_{-\infty}^{\infty}e^{-j2\pi(F_n-f_s)t}w_m(t)e^{j(\theta(t)+\phi_n(t))}\,\mathrm{d}t \\ &+ \int_{-\infty}^{\infty}z_m(t)e^{-j2\pi F_n t}e^{j\phi_n(t)}\,\mathrm{d}t = \sum_{s=0}^{S-1}a_s\tilde{G}_{s,m}(F_n) + \tilde{Z}_m(F_n), \quad (19)\end{aligned}$$

where $\tilde{G}_{s,m}(F_n)=H(f_s)\int_{-\infty}^{\infty} e^{-j2\pi(F_n-f_s)t} w_m(t) e^{j(\theta(t)+\phi_n(t))} \mathrm{d}t$. The above expression reduces to

$$R_m(F_n) = \sum_{s=0}^{S-1} H(f_s) a_s e^{j(\Phi_n+\Theta)} G_{s,m}(F_n - (\delta f_n + \delta \bar{f})) + \tilde{Z}_m(F_n), \tag{20}$$

where $G_{s,m}(F)$ is given by (14). Thus, frequency offset introduces a constant complex phase equal to $\Phi_n + \Theta$ and an offset in the frequency sample equal to $\delta F_n = \delta f_n + \delta \bar{f}$.

In order to provide simulation results, a multicarrier communication system example is implemented, where the purpose of the simulation is to compare conventional and proposed scheme under frequency mismatch. A transmission rate of $R = 250$ Mbps is desired, which will be achieved by transmitting 125 binary modulated carriers with frequency spacing of 4 MHz in a 500 MHz bandwidth that lies in the range 3.1 GHz - 3.6 GHz. Moreover, since the desired transmission rate is $R = 250$ Mbps, 125 bits are transmitted every $T = 500$ ns. Additionally, for simplicity we assumed an AWGN channel. Figure 4 (a) shows the signal to noise ratio (SNR) vs. the fractional frequency offset $\delta F_n/F_n$ (it is assumed that $\Phi_n + \Theta = 0\ \forall n$ for simplicity) for both a conventional digital multicarrier receiver implemented with a single oscillator that shifts the received signal to baseband followed by ADC in time domain at Nyquist rate (1 GHz), and the proposed multicarrier receiver with ADC in frequency domain and conversion-time $T_c = T/M = 20$ ns, which requires 10 multiply and integrate devices operating at 50 MHz. This figure shows that the new receiver not only relaxes the operational speed of the A/D conversion but also performs better than the traditional implementation of digital multicarrier receivers for the same conditions of frequency offset. This important advantage can be explained by observing that by using a conversion-time T_c that is smaller than the symbol-period T, the spectrum of each one of the segmented received signals is spread out providing some degree of robustness to variations in the frequencies at which the frequency domain ADC samples the received signal. Additionally, Fig. 4 (b) provides a similar conclusion in terms of bit error rate (BER) vs. $\mathrm{SNR}_{\mathrm{AWGN}} = 10\log_{10}(E_b/N_o)$, parameterized by several fractional frequency offsets, where E_b is the total transmitted power per information bit.

V. Conclusions

This paper introduces a multicarrier communication receiver based on analog to digital conversion of the received signal in the frequency domain. The proposed receiver architecture channelizes the spectrum of the received signal by taking N samples of it every $\Delta F_c = 1/T_c$ Hz, where T_c is the A/D conversion-time. The receiver allows for a proper design of the parameters T_c and N, which determines the speed and the system complexity. The favorable trade-off between T_c and N provides a solution to the challenging problems found in the analog to digital conversion needed at the receive end of high-speed communications systems that use signals with very large bandwidths. The proposed receiver possesses advantages of great interest in broadband communication systems including robustness to frequency offset. Narrow band interference rejection methods that exploit the time-frequency resolution provided by the frequency domain ADC may also be implemented.

References

[1] R. W. Chang, "Orthogonal frequency divison multiplexing," *U.S. Patent 3,488,445, issued Jan. 6 1970*.

[2] B. R. Saltzberg, "Performance of an efficient data transmision system," *IEEE Trans. Commun. Technol.*, pp. 805–813, Dec. 1967.

[3] I. Kalet, "The multitone channel," *IEEE Transactions on Communications*, pp. 119–124, Feb. 1989.

[4] P. S. Chow, J. M. Cioffi, and J. A. C. Bingham, "A practical discrete multitone transceiver loading algorithm for data transmission over spectrally shaped channels," *IEEE Transactions on Communications*, pp. 773–775, Feb.-March 1995.

[5] L. J. Cimini, Jr., "Analysis and simulation of a digital mobile channel using orthogonal frequency division multiplexing," *IEEE Transactions on Communications*, pp. 665–675, Jun. 1985.

[6] S. B. Weistein and P. M. Ebert, "Data transmission by frequency-division multiplexing using the discrete Fourier transform," *IEEE Trans. Commun. Technol.*, vol. COM-19, pp. 628–634, Oct. 1971.

[7] B. Hirosaki, "An orthogonally multiplexed QAM system using the discrete Fourier transform," *IEEE Transactions on Communications*, vol. COM-29, pp. 928–989, Jul. 1981.

[8] "Revision of part 15 of the commission's rule regarding ultra-wideband transmission," *Federal Communications Commission*, 1st Rep. and Order, 2002.

[9] J. Balakrishnan, A. Batra, and A. Dabak, "A multi-band OFDM system for UWB communication," *Proceedings of UWBST 2003, IEEE Conference on Ultra Wideband Systems and Technologies, Reston, VA, 2003.*, Nov. 2003.

[10] S. Hoyos, B. M. Sadler, and G. R. Arce, "Analog to digital conversion of ultra-wideband signals in orthogonal spaces.," *Proceedings of UWBST 2003, IEEE Conference on Ultra Wideband Systems and Technologies, Reston, VA, 2003.*, Nov. 2003.

[11] S. Hoyos, B. M. Sadler, and G. R. Arce, "High-speed A/D conversion for ultra-wideband signals based on signal projection over basis functions.," *Proceedings of ICASSP 2004, International Conference on Acoustics, Speech and Signal Processing, Montreal, Quebec, Canada, 2004.*, 2004.

[12] H-J Lee, D. S. Ha, and H-S Lee, "A frequency-domain approach for all-digital CMOS ultra-wideband receivers," *Proceedings of UWBST 2003, IEEE Conference on Ultra Wideband Systems and Technologies, Reston, VA, 2003.*, Nov. 2003.